

***Zanthoxylum avicennae* extracts induce cell apoptosis through protein phosphatase 2A activation in HA22T human hepatocellular carcinoma cells and block tumor growth in xenografted nude mice**

TRAN DUC DUNG¹, HSIEN-CHEH CHANG¹, CHUNG-YU CHEN², WEN-HUANG PENG³, CHANG-HAI TSAI⁴, FUU-JEN TSAI¹, WEI-WEN KUO⁵, LI-MIEN CHEN^{6,7} and CHIH-YANG HUANG^{1,8,9}

¹School of Chinese Medicine, China Medical University, Taichung; ²Department of Chemistry, National Chung Hsing University, Taichung; ³Graduate Institute of Chinese Pharmaceutical Sciences, China Medical University, Taichung; ⁴Department of Healthcare Administration, Asia University, Taichung; ⁵Department of Biological Science and Technology, China Medical University, Taichung; ⁶Division of Medical Technology, Department of Internal Medicine, Armed-Forces Taichung General Hospital, Taichung; ⁷Center of General Education, Central Taiwan University of Science and Technology, Taichung; ⁸Graduate Institute of Basic Medical Science, China Medical University, Taichung; ⁹Department of Health and Nutrition Biotechnology, Asia University, Taichung, Taiwan, R.O.C.

Received June 6, 2011; Accepted July 18, 2011

DOI: 10.3892/ijmm.2011.780

Abstract. The use of herbs as alternative cancer therapies has attracted a great deal of attention owing to their lower toxicity. Whether *Zanthoxylum avicennae* (Ying Bu Bo, YBB) induces liver cancer cell apoptosis remains unclear. In this study, we investigated the effect of YBB extracts (YBBEs) on HA22T human hepatocellular carcinoma cells *in vitro* and in an *in vivo* mouse xenograft model. HA22T cells were treated with different concentrations of YBBEs and analyzed with Western blot analysis, TUNEL, JC-1 staining and siRNA transfection assays. Additionally, the HA22T-implanted xenograft nude mice model was applied to confirm the cellular effects. YBBEs-induced apoptosis, up-regulated death receptor apoptotic pathway markers as well as mitochondrial proteins, and suppressed the survival proteins in a dose-dependent manner. Pro-survival Bcl-2 family proteins were inhibited and the pro-apoptotic ones were increased. Protein phosphatase 2A (PP2A) siRNA or okadaic acid reversed the YBBEs effects, confirming the role of PP2A in YBBEs-induced HA22T apoptosis. All our experimental evidence indicates that YBBEs significantly promote HA22T apoptosis and reduce tumor sizes in xenograft nude mice via PP2A in a dose-dependent manner.

Introduction

Hepatocellular carcinoma (HCC) is the fifth most common disease worldwide and the third cause of cancer-related deaths (1,2). Apoptosis is a morphologically defined mode of cell death characterized by nuclear condensation and fragmentation, membrane blebbing and the formation of apoptotic bodies (3). Until now, apoptosis induction by various cytotoxic anti-cancer agents has been one of the most effective cancer therapy methods (4-7). Recently, some herbs have been shown to be potent cancer-protective or cancer-preventive agents against chemical-induced carcinogenesis *in vitro* and *in vivo* (8-10). The use of these herbs as alternative cancer therapies has attracted a great deal of attention owing to their lower toxicity as well as cost benefit. *Zanthoxylum avicennae* (Ying Bu Bo, YBB), a traditional Vietnamese herb, has been widely used to treat icterohepatitis, jaundice, edema due to nephritis and rheumatoid arthritis (11-14). In addition, YBB is also used to treat hepatitis B, hepatocirrhosis, colitis and stomatitis in Vietnamese folk medicine.

Protein phosphatase 2A (PP2A) is a phosphatase with tumor suppressor activity and it has been indicated that pharmacological enhancement of PP2A represents a possible therapeutic strategy (15). However, the anti-tumor and pro-apoptotic mechanisms of YBB on human HCC are still not clearly understood. This study was designed to investigate whether YBB extracts (YBBEs) could induce apoptosis in HA22T cells and then to investigate the molecular mechanisms of its anti-cancer properties in both *in vitro* and *in vivo* models.

Materials and methods

Cell culture. HA22T cells (BCRC no. 60168) were obtained from Bioresources Collection and Research Center, Food

Correspondence to: Dr Chih-Yang Huang, Graduate Institute of Basic Medical Science, School of Chinese Medicine, China Medical University and Hospital, 91 Hsueh-Shih Road, Taichung 404, Taiwan, R.O.C.
E-mail: cyhuang@mail.cmu.edu.tw

Key words: hepatocellular carcinoma, *Zanthoxylum avicennae* (Ying Bu Bo), protein phosphatase 2A, apoptosis, nude mice

Industry Research and Development Institute (Hsinchu, Taiwan), and were cultured in Dulbecco's modified Eagle's medium (DMEM) supplemented with 10% FBS. Cells were seeded in cell culture flasks and were maintained in a humidified incubator at 37°C with 5% CO₂.

Animals. About 20 male NU/NU nude mice of 20–22 g in weight, 5 weeks in age were obtained from BioLASCO Taiwan Co., Ltd. (Taipei, Taiwan) and were given food and water *ad libitum*. The NU/NU nude mice were maintained at the China Medical University Animal Center for 2 weeks under guidelines for the use of animals before grouping and initiating the experiments. Mice were housed in a room maintained at 25±1°C with 55% relative humidity.

Ying Bu Bo extraction. Bark (850 g) from YBB roots was washed with water 3 times followed by immersion in 95% alcohol. After 2 days, the extract was filtered with gauze. This step was repeated 4 times. The extract was then dried in a baking oven at 40–45°C. This process provided 61.93 g of crude extract from YBB-Root bark (shorten as YBBEs). The extraction rate was 7.29%. The extract was kept in a humid cabinet. From this step onward, the YBBEs were dissolved in distilled water and then filtered through a 0.22 µm microspin filter just prior to the experiments. According to the experimental design, the HA22T cell line was incubated with 0, 50, 100, 150, 200 and 250 µg/ml of the extract for 24 h. The dose for the animal experiments was 20 or 40 mg/kg YBBEs.

Chromatographic analysis of YBBEs. A mixture of YBBEs, Hesperidin and Diosmin and Hesperidin were dissolved in 50% methanol solution (water:methanol, 1:1) and then filtered through a 0.2 µm Nylon 66 filter. An Agilent 1100 series liquid chromatography system consisting of a binary solvent delivery system and UV-Vis variable multi-wavelength detector (Agilent Technologies, Inc., Palo Alto, CA, USA) was used. The HPLC system consisted of a Waters XTerra RP18 (4.6x250 mm, 5 µm particle size; Waters Corp., Milford, MA). The flow rate was 0.7 ml/min, the sample loop was 5 µl and the detection wavelength was 254 nm. A gradient elution was used, starting at 20% solvent B, changing to 50% solvent B for 15 min, then changed to 70% for 25 min and held until the end of the gradient. The YBBEs, Hesperidin, and Diosmin sample mixture peaks were identified by comparison with a standard solution (Hesperidin pure compounds). The 50% methanol solutions were quantified by spiking with a known amount of standard and also by comparing the area under the curve.

Cell morphological changes determinations. HA22T cells were grown in 6-well plates (at a density of 5x10⁵ cells/well) containing DMEM for 24 h. For dose-response experiments, different concentrations of YBBEs (0, 50, 100, 150, 200 and 250 µg/ml) were incubated in humidified air with 5% CO₂ at 37°C for 24 h. At the end of each incubation period, cells were fixed with 4% paraformaldehyde for 20 min. After washing with PBS, photographs were taken to record the morphological changes of HA22T cells using an inverted fluorescent microscope.

TUNEL assay. The HA22T cells were cultured in a 24-well plate (5x10⁴ cells/well) with different concentrations of YBBEs

(0, 50, 100, 150, 200, 250 µg/ml) at 37°C for 24 h. The cells were rinsed 5 times with PBS and fixed in 4% paraformaldehyde solution at room temperature for 1 h. The fixed cells were pre-treated with blocking buffer (3% H₂O₂ in methanol) for 10 min at room temperature. After a rinse with PBS, cells were treated with permeation solution (0.1% Triton X-100 in 0.1% sodium citrate) for 2 min at 4°C. Next, following washing with PBS, 10X diluted TUNEL reagent (enzyme solution and label solution) (In Situ Cell Death Detection kit, Fluorescein, Roche, Germany) was added and the plate was placed in humidified air at 37°C for 1 h for the reagent to react with cell nuclei. DAPI diluted 10,000X per well was added and the plate was covered with tin foil and rested for 25 min. Finally, the cells were observed with fluorescent microscopy.

Western blot analysis. HA22T cells were scraped and washed once with phosphate-buffered saline (PBS). Cell pellets were lysed for 30 min in lysis buffer and spun down at 12,000 x g for 10 min. Tissue samples were homogenized with ice-cold PBS and then subjected to lysis in a solution containing 20 mM Tris, 2 mM EDTA, and 1% glycerol. Supernatants were obtained after centrifugation at 12,000 x g for 40 min. After boiling, proteins were separated on a 12% SDS-PAGE gel with a constant voltage of 75 V for 2.5 h, and proteins were then transferred to a polyvinylidene difluoride (PVDF) membrane with a transfer apparatus at a constant voltage of 100 V for 2 h. Membranes were blocked with 5% nonfat milk in 0.05% Tween-20 in PBS for 1 h at room temperature and then incubated with primary antibody. The membranes were washed with 10 mM Tris, 150 mM NaCl, and 0.05% Tween-20 and incubated with secondary antibody (goat anti-mouse IgG at 1:2,000). The immunoblotted proteins were visualized using an ECL Western blot analysis luminal reagent and quantified using a Fujifilm LAS-3000 chemiluminescence detection system (Fujifilm, Tokyo, Japan).

JC-1 staining. JC-1 (5,5',6,6'-tetrachloro-1,1',3,3'-tetraethylbenzimidazol-carbocyanine iodide) is a lipophilic fluorescent cation that can incorporate into the mitochondrial membrane, where it can form aggregates due to the physiological membrane potential state of the mitochondria. Briefly, HA22T cells were cultured in a 6-well plate (2x10⁴ cells/well) with different concentrations of YBBEs (0, 50, 100, 150, 200, 250 µg/ml) at 37°C for 24 h. The cells were washed three times with PBS and incubated with medium containing JC-1 staining reagent at 37°C for 20 min followed by washing with PBS. The stained cells were examined under an Olympus CKX41 fluorescence microscope. JC-1 formed aggregates in the apoptotic mitochondria while it remained a monomer in the normal mitochondria.

Gene knockdown using siRNA. HA22T cells were seeded into 6-wells plates and grown to 80%. siRNA transfection was carried out with DharmaFECT Duo transfection reagent (Dharmacon, Inc.). The 100 µl PP2A-Cα siRNA (Santa Cruz Biotechnology, Inc., Santa Cruz, CA) and 100 µl negative control transfect Non-Targeting Pool (NT) (Dharmacon, Inc., Lafayette, CO) were mixed with 100 µl serum-free medium. At the same time, a sufficient amount of DharmaFECT Duo reagent was diluted to 1:50 in serum-free medium and incubated for 5 min at room temperature. The two mixtures

were combined by careful pipetting and the plates were incubated at 37°C for 20 min to allow for transfection complex formation. After adding sufficient serum-free medium for 24 h, the serum-free medium was removed and then cultured with a medium containing 10% fortified bovine calf serum. Cells were incubated at 37°C in 5% CO₂, and then harvested 48-96 h post-transfection for protein expression analysis. Specific silencing was confirmed by immunoblotting with cellular extracts 72 h after transfection.

Liver cancer tumor model. The NU/NU nude mice were divided into three groups with each group containing six animals. In group I, HA22T cells (1x10⁶ in 100 µl DMEM) were subcutaneously injected into the left flank of NU/NU mice as a control. Group II was injected with HA22T cells and orally treated with 20 mg/kg YBBEs in water. Group III was injected with HA22T cells and orally treated with 40 mg/kg YBBEs in water.

Four days after tumor inoculation, mice were given daily oral treatment with YBBEs. Tumor volumes were measured every three days with a caliper and calculated according to the formula $[(L \times W^2)/2]$, where L and W indicate the length and width, respectively (16). All mice were sacrificed 15 days after tumor inoculation. The tumors were excised and weighed.

Immunohistochemistry. Tissue specimens from sacrificed NU/NU mice were collected and immediately fixed in 10% buffered formalin overnight, embedded in paraffin, and sectioned to 4 µm thickness. The tumor sections were immobilized and deparaffinized by immersing in xylene, dehydrated in a graded series of ethanol and washed with distilled water. For antigen retrieval, the tumor sections were boiled in 0.1% sodium citrate (in 0.1% Triton X-100) for 10 min at 4°C. Next, following washing twice with PBS, endogenous peroxidase activity was blocked by incubation in 3% H₂O₂-methanol for 10 min at room temperature. The sections were stained with antibodies for proliferating cell nuclear antigen PCNA and caspase-3 overnight at 4°C. Terminal deoxynucleotidyl transferase-mediated dUTP nick end labeling (TUNEL) staining was performed using a TACS™ 2 TdT-DAB In Situ Apoptosis Detection kit (Gaithersburg, MD, USA). Images were taken using an inverted Olympus CKX41 fluorescence microscope. Proliferative index (%) = (no. of PCNA positive cells/total cells) x 100. Apoptotic index (%) = (no. of caspase-3 positive cells/total cell) x 100 = (no. of TUNEL positive cells/total cell) x 100.

Statistical analysis. Each sample was analyzed based on results that were repeated at least three times using the SigmaPlot 10.0 software. Results were presented as mean ± SE, and the statistical comparisons were made using the Student's t-test. In all cases, differences at p<0.05 were regarded as statistically significant, those at p<0.01 or p<0.001 were considered to have higher statistical significance.

Results

Chromatographic analysis of the YBBEs, Hesperidin, and Diosmin and HPLC of Hesperidin mixture. The presence

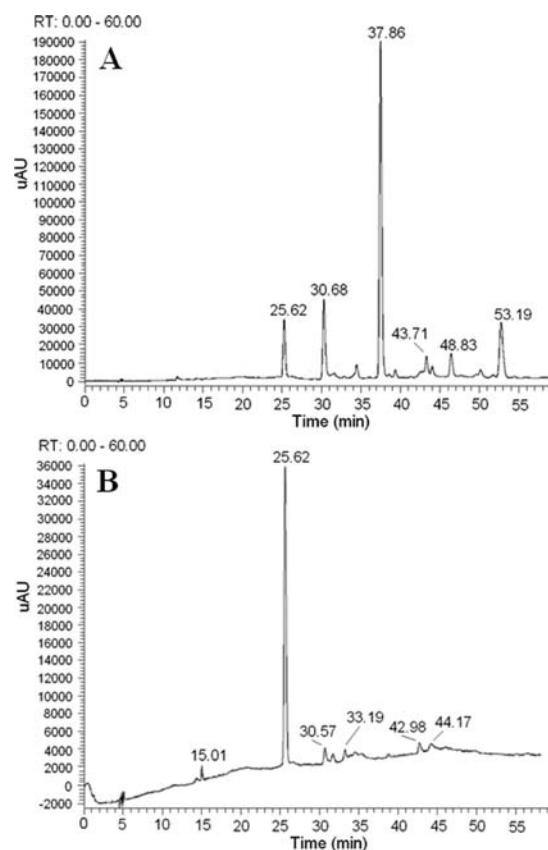


Figure 1. HPLC chromatographic profile of (A) mixture of YBBEs, Hesperidin, and Diosmin and (B) Hesperidin. $\lambda=254$ nm for Hesperidin.

of functional components in YBBEs such as flavonoids is believed to be responsible for the beneficial effects. However, the amount and variety of flavonoids in YBBEs still remains unknown. This study developed a high performance liquid chromatography (HPLC) method for Hesperidin determination in YBBEs. Chromatographic analysis of the YBBEs, Hesperidin and Diosmin mixture is shown in Fig. 1A. The HPLC chromatogram of Hesperidin, the major component among the organic molecules of YBBEs is shown in Fig. 1B, which has a maximum absorbance at 254 nm. This analytical result indicates the Hesperidin content is 75 mg per 1 g YBBEs.

Induction of apoptosis by YBBEs in HA22T cells. HA22T cells were treated with various doses of YBBEs. As shown in Fig. 2A, untreated HA22T cells grew well with clear skeletons, while cells treated with YBBEs, were distorted and some became rounded. The floating cells increased with increasing drug concentrations.

To confirm the morphological changes in the apoptosis data DNA fragmentation was then detected using the *in situ* DNA labeling TUNEL assay, which is a very sensitive indicator of apoptosis. As shown in Fig. 2B, approximately 1.00, 4.33, 19.33, 22.67, 25.67 and 46.66% TUNEL-positive cells (apoptotic cells) were observed after 24 h of YBBEs treatment. The data from the TUNEL assay also support that treatment with YBBEs induced apoptotic cell death in human hepatoma cell lines.

YBBEs induce apoptosis in HA22T cells through the death receptor and mitochondria-dependent apoptotic pathway.

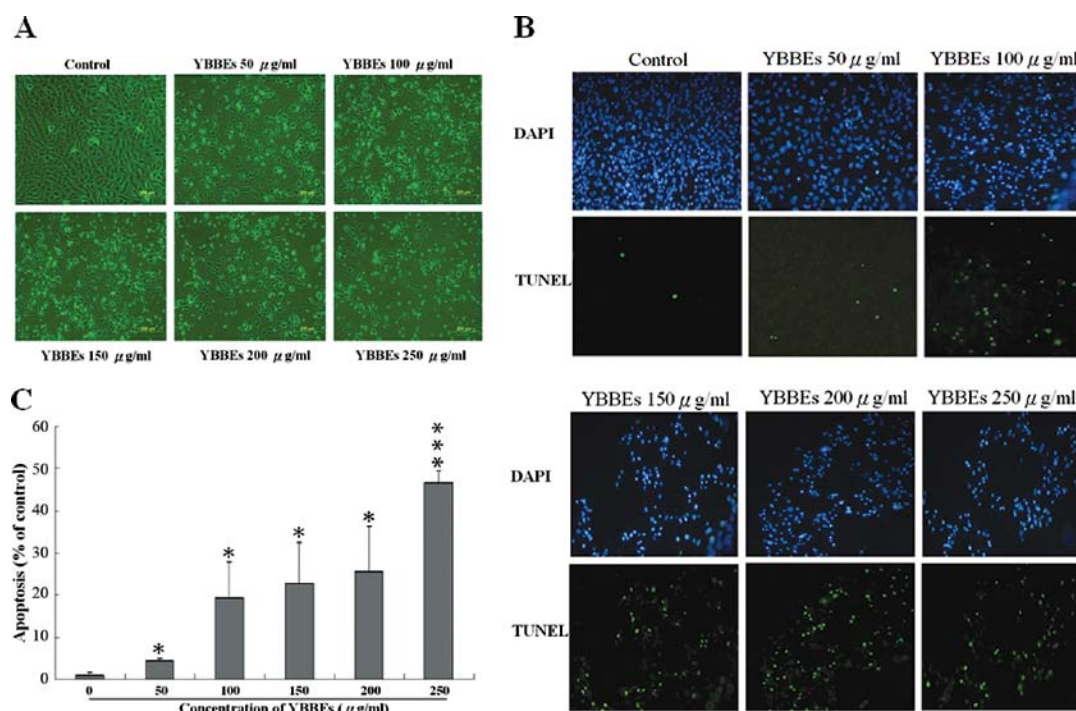


Figure 2. YBBEs induce apoptosis in human HA22T liver cancer cells. The HA22T cells were treated with different concentrations of YBBEs (0, 50, 100, 150, 200 and 250 µg/ml) for 24 h. (A) The morphological changes of viable HA22T cells after treatment with YBBEs. Photographs were taken on the morphological changes of HA22T cells and then observed under an inverted light microscope. (B) DAPI was used to label nuclei (upper panels) and apoptotic cell nuclei were labeled by TUNEL stain (lower panels). (C) Partition of positive apoptotic cells was based on percentages calculated from three sections of each treatment as described in Materials and methods. Data are presented as mean \pm SEM. * $p < 0.05$ and *** $p < 0.001$ values based on comparisons with untreated controls.

Western blot analysis was carried out to detect the death receptor-dependent protein expressions. After treatment of HA22T cells with YBBEs for 24 h, the levels of tumor necrosis factor (TNF) α , TNF-R1, FAS-L, FAS, FADD, caspase-8, BID and t-BID were markedly increased (Fig. 3A). These results revealed that the death receptor-dependent apoptotic pathway had an important role in YBBEs-induced apoptosis in HA22T cells. Accordingly, we further examined the YBBEs effect on the Bcl-2 family proteins, essential components of the apoptosis pathways. As shown in Fig. 3C exposure of HA22T cells to YBBEs for 24 h markedly increased the protein expression of the pro-apoptotic Bax, Bak, Bad with a concomitant decrease in the expression of the anti-apoptotic Bcl-2, Bcl-xL, p-Bad proteins time-dependently, compared with the untreated control, thereby the Bax/Bcl-2 ratio would be increased (Fig. 3D). Based on these findings, it can be concluded that YBBEs induced apoptosis in HA22T cells through modulation of the Bcl-2 family.

In addition, we also examined whether the mitochondrial-mediated apoptotic pathway was involved in YBBEs-induced apoptosis. As shown in Fig. 3E, YBBEs promoted the levels of cytochrome c, caspase-9 and caspase-3. Since apoptosis inducing factor (AIF) protein is one of death protein candidates that serves in the mitochondrial-related caspase-independent pathway (17,18) we investigated whether the AIF protein was involved in the cell death induced by YBBEs. In our experiments, the level of AIF protein expression was significantly increased after the treatment of HA22T cells with 0, 50, 100, 150, 200 and 250 µg/ml YBBEs for 24 h (Fig. 3E).

These observations imply that translocation of AIF from the mitochondria into the cytosol plays an important role in the early stages of the apoptotic process and confirm that

this apoptosis pathway is involved in mitochondrial function. Moreover, it is possible that the caspase-independent apoptotic pathway via the translocation of AIF protein from the mitochondria into the cytosol may also be activated by YBBEs treatment. Mitochondria permeability transition results in the release of cytochrome c from the mitochondrial internal space into the cytoplasm (19). Treatment with YBBEs at concentrations greater than 50 µg/ml induced the cytoplasmic release of cytochrome c, confirming the activation of the mitochondria-dependent pathway. This result suggests that YBBEs induces apoptosis in human liver cancer cells through the mitochondria-dependent pathway.

The mitochondrial membrane depolarization and the associated mitochondria damage was evaluated using JC-1 staining. When ETC functions abnormally, the mitochondrial membrane potential becomes unstable and JC-1 appears as a JC-1 monomer, which emits at 530 nm and can be detected with FITC (green). This indicates a mitochondrial outer membrane permeabilization (MOMP) event in a cell. Changes in Cy3 (red) and FITC emission intensities can be used to detect changes of mitochondrial membrane potential and therefore changes of the cellular metabolic state. In control cells (i.e. no drug treatment), there were only strong Cy3 signals and no FITC (Fig. 3G). Administration of 50, 100, 150, 200 and 250 µg/ml YBBEs resulted in weak Cy3 signals and an increase in FITC signals. It is thus concluded that YBBEs treatment significantly decreased the mitochondrial membrane potential of HA22T cells in a dose-dependent manner.

Effects of YBBEs on the survival pathway of HA22T cells. To further study the suppressed effect of YBBEs on the IGF-I

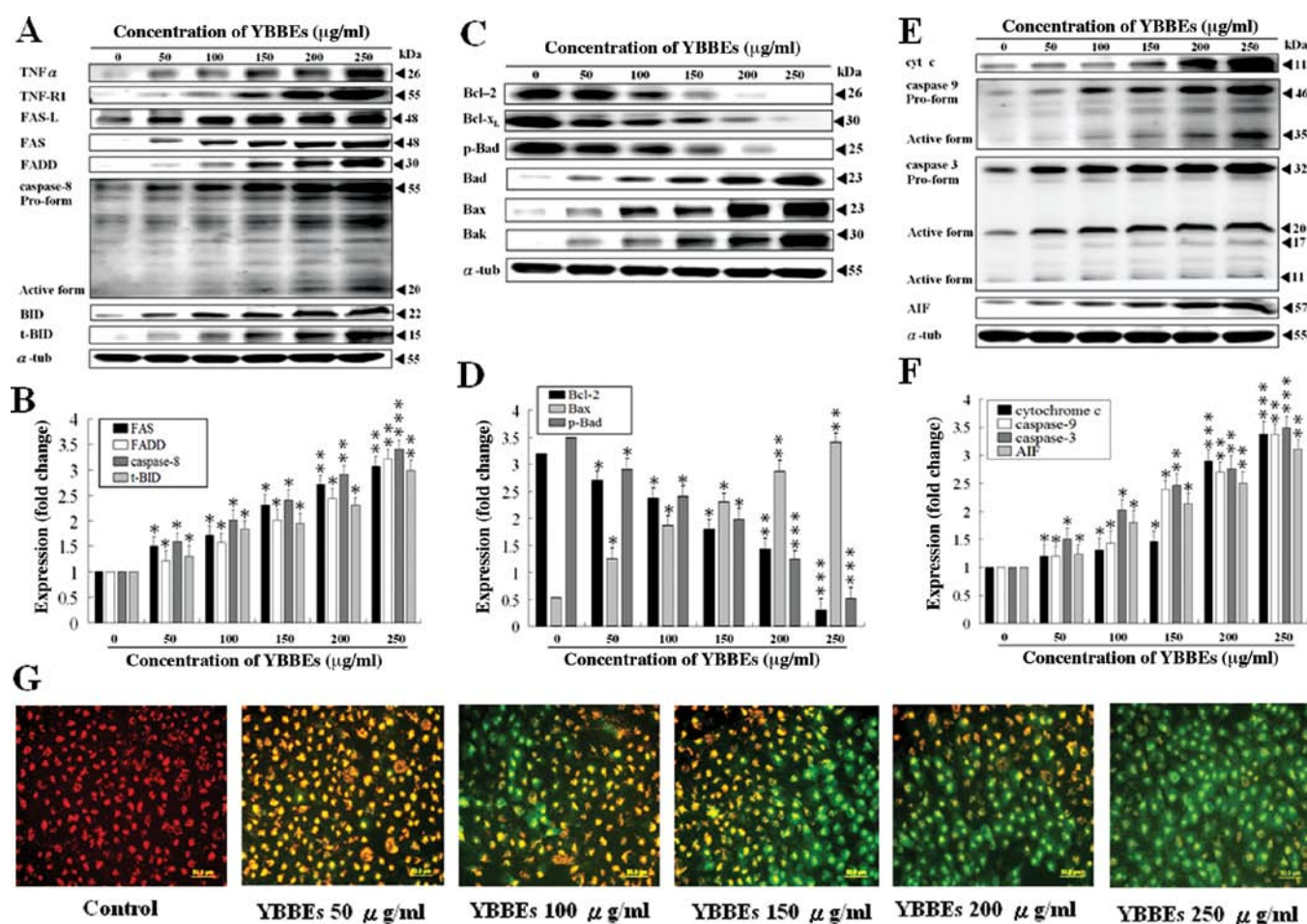


Figure 3. Effects of YBBEs on death receptor-dependent and mitochondria-dependent apoptotic pathways in the human hepatoma cell line, HA22T. HA22T cells were cultured in the presence of different concentrations of YBBEs for 24 h and then the total protein samples were obtained. (A) TNF α , TNF-R1, FAS-L, FAS, FADD, caspase-8, BID and t-BID levels were examined by Western blot analysis. (B) Bars represent the relative quantification of FAS, FADD, caspase-8 and t-BID on the basis of control level. (C) Regulation of the Bcl-2 family proteins by YBBEs. (D) Bars represent the relative quantification of Bcl-2, Bax and p-Bad on the basis of control level. (E) The protein expression levels of cytochrome c (cyt c), caspase-9, caspase-3 and apoptosis inducing factor (AIF) were measured by Western blotting. (F) Bars represent the relative quantification of cyt c, caspase-9, caspase-3 and AIF compared to the control. Equal loading was assessed with an anti- α -tubulin antibody. Cells cultured without treatments were used as control. The quantitative results are expressed as the mean value \pm SE (n=3). *p<0.05, **p<0.01 and ***p<0.001 vs. the control group (line 1). (G) The effects of YBBEs mitochondrial outer membrane permeabilization (MOMP) on HA22T cells. FITC (green) signals represent unstable mitochondrial outer membrane permeabilization (MOMP) and Cy3 (red) signals represent normal mitochondrial membrane permeability. Comparison of the ratio of green and red images implies the damage degree of MOMP on HA22T cells.

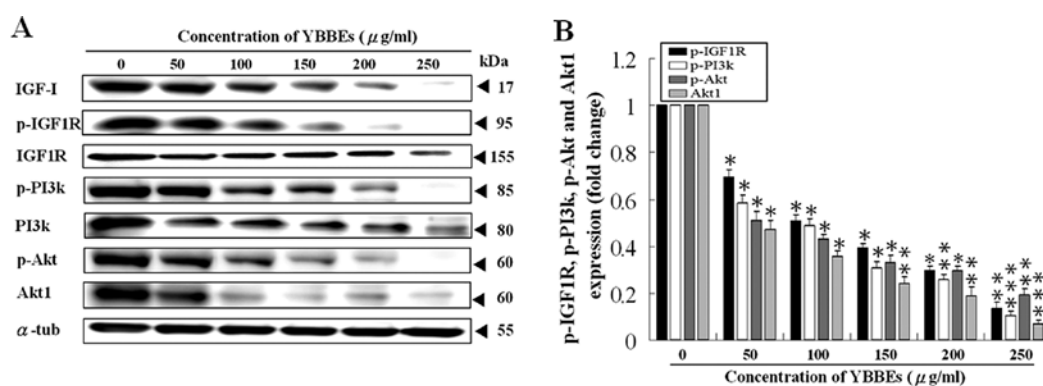


Figure 4. YBBEs suppressed the IGF-I cell survival pathway. (A) The protein expression levels (IGF-I, p-IGF1R, IGF1R, p-PI3k, PI3k, p-Akt and Akt) were measured by Western blotting. α -tubulin was used as an internal loading control to confirm equal loading. (B) Bars represent the relative quantification of p-IGF1R, p-PI3k, p-Akt and Akt1 on the basis of control level. The quantitative results are expressed as the mean value \pm SE (n=3). *p<0.05, **p<0.01 and ***p<0.001 vs. the control group (line 1).

survival pathway in HA22T cells, Western blot analysis was performed. The protein expression analysis of IGF-I, p-IGF1R,

IGF1R, p-PI3k and PI3k in control and YBBEs-treated HA22T cells is shown in Fig. 4A. Compared to the control, five

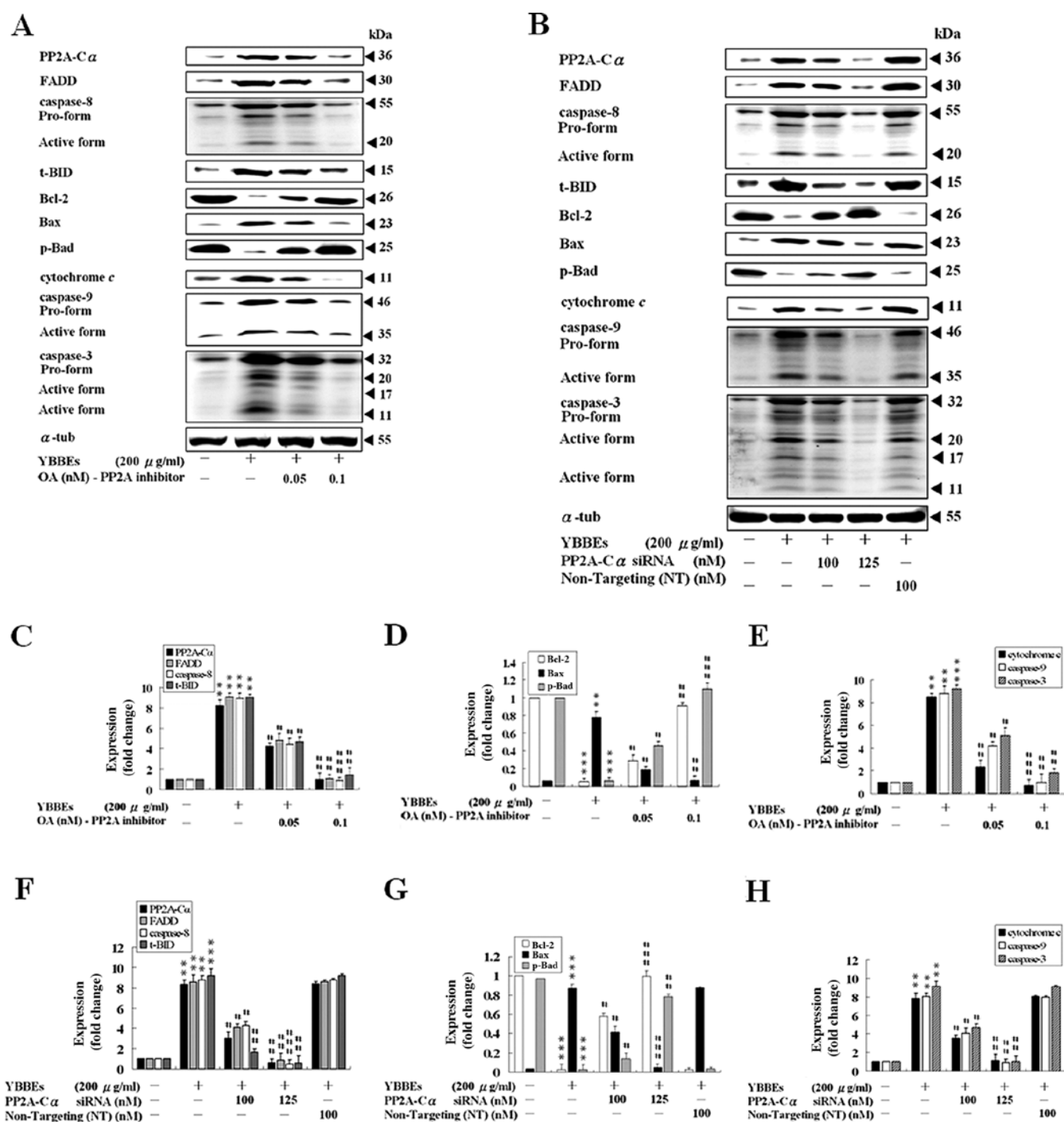


Figure 5. YBBEs induce cell apoptosis through PP2A activation in HA22T cells. HA22T cells were treated with okadaic acid (OA), a PP2A inhibitor (0.05 and 0.1 nM for 1 h) or 100 and 125 nM PP2A-C α siRNA and 100 nM control non-targeting (NT) siRNA and then subsequently treated with YBBEs (200 μ g/ml) for another 24 h. (A) OA blocks YBBEs-induced HA22T cell apoptosis by inhibiting the expression of PP2A-C α by Western blot analysis. (B) PP2A-C α siRNA inhibits YBBEs-induced HA22T cell apoptosis by Western blot analysis. α -tubulin was used as a loading control. (C and F) Bars represent the relative quantification of PP2A-C α , FADD, caspase-8 and t-BID on the basis of the control level. (D and G) Bars represent the relative quantification of Bcl-2, Bax and p-Bad on the basis of the control level. (E and H) Bars represent the relative quantification of cytochrome c (cyt c), caspase-9 and caspase-3 on the basis of the control levels. The quantitative results are expressed as the mean value \pm SE (n=3). **p<0.01 and ***p<0.001 denotes significant differences from control values with YBBEs treatment. #p<0.05, ##p<0.01 and ###p<0.001, denote significant differences from YBBEs treatment of OA or siRNA.

different doses of YBBEs resulted in significant decreases of IGF-I, p-IGF1R, IGF1R, p-PI3k and PI3k in a dose-dependant manner. In mammalian cells, the serine/threonine protein kinase AKT is widely recognized as a key mediator of growth factor to promote cell survival, and recent evidence indicates that AKT is often constitutively active in many types of human

cancer (20). We used Western blot analysis to examine the phosphorylation status of AKT, which is crucial for its kinase activity. The analysis revealed that in HA22T cells, the level of phospho-Akt and Akt1 decreased significantly during incubation with YBBEs for 24 h and the corresponding band almost disappeared at 250 μ g/ml (Fig. 4A). Our study provides strong

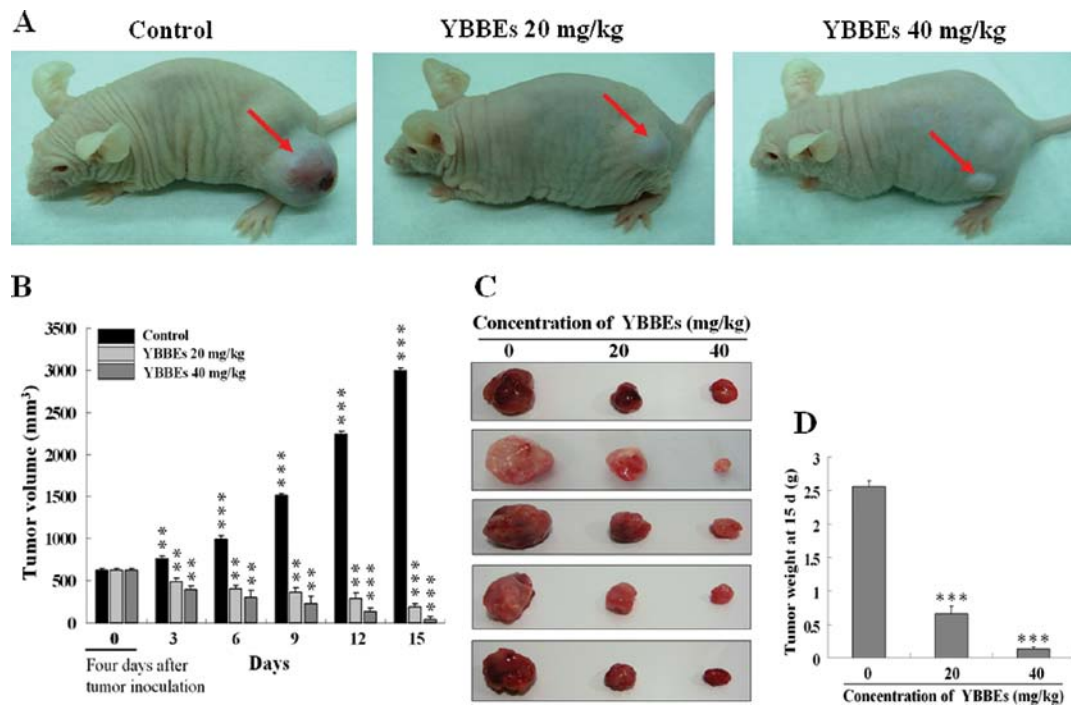


Figure 6. Effect of YBBEs on the growth of xenografted HA22T tumor tissue in nude mice. HA22T cells (1×10^6 in $100 \mu\text{l}$ DMEM) were subcutaneously injected into the left flank of NU/NU mice. Starting at four days after inoculation, when the tumors had reached a volume around 600 mm^3 , mice were orally treated with YBBEs (20 or 40 mg/kg) every day. For tumor size measurements, the length (L) and width (W) of the tumor were measured with calipers, and tumor volume (TV) was calculated as $\text{TV} = (\text{L} \times \text{W}^2)/2$. Tumors of all sacrificed mice 15 days after HA22T inoculation were removed, photographed and weighed. (A) Representative pictures of drug-treated hepatomas. Red arrows indicate tumor mass. (B) Effect of YBBEs on final tumor volumes. (C) Photographic records of final harvested tumors. (D) Effect of YBBEs on final tumor weight. Data were expressed as means \pm SE, $n=5$. The statistically significant differences compared with control were calculated by the Student's t-test (* $p<0.05$, ** $p<0.01$ and *** $p<0.001$).

evidence that YBBEs extraction inhibits survival pathway in human HCC cells.

Okadaic acid (OA) inhibits YBBEs-induced apoptosis mediated through the down-regulating of PP2A-C α in HA22T cells. We further determined the roles of PP2A on the YBBEs-inhibited HA22T cell proliferation. HA22T cells were pre-treated with OA, a pharmacological inhibitor of PP2A, followed by treatment with $200 \mu\text{g/ml}$ YBBEs for 24 h.

YBBEs ($200 \mu\text{g/ml}$) treatment significantly inhibited the expression of Bcl-2 and p-Bad, and accompanied with an increased of PP2A-C α , FADD, caspase-8, t-BID, cyt c, caspase-9, caspase-3 and Bax expression. However, this situation was totally reversed after treating with OA in the presence of YBBEs (Fig. 5A).

PP2A-C α siRNA blocks YBBEs-induced apoptosis in HA22T cells. To further confirm that YBBEs induce HA22T cell apoptosis through PP2A, we transfected HA22T cells with PP2A-C α siRNA. Results from the Western blot analysis assay showed a significant reduction in the PP2A-C α , FADD, caspase-8, t-BID, Bax, cyt c, caspase-9, caspase-3 proteins level in HA22T cells, accompanied with the increased protein level of Bcl-2 and p-Bad (Fig. 5B). Therefore, our results strongly suggested that PP2A is an important mediator of YBBEs-induced HA22T cell apoptosis.

YBBEs suppress tumor growth in vivo. We further examined whether the strong anti-proliferative and apoptosis effects of

YBBEs detected in cell culture experiments, could be observed in an *in vivo* model.

NU/NU mice bearing subcutaneously implanted HA22T cells were given a daily oral dose of YBBEs. In a pilot study, we used 20 and 40 mg/kg of YBBEs in an *in vivo* study. The growth of HA22T xenografts was monitored every three days for 2 weeks. Side effects, such as body weight loss, mortality and lethargy were not observed in mice treated with YBBEs for 2 weeks. The final tumor size, as shown in Fig. 6A and B, was markedly smaller in the majority of mice treated with 20 or 40 mg/kg of YBBEs. The tumor weight was significantly suppressed by treatment with YBBEs at these doses (Fig. 6C and D), and the overall data suggest a trend for a dose-response. The most effective anti-hepatoma response was elicited at 40 mg/kg of YBBEs. These results strongly indicate that YBBEs suppress tumor growth *in vivo*.

YBBEs inhibit tumor cell proliferation and increase tumor cell apoptosis in vivo. To assess the anti-proliferative effect of YBBEs *in vivo*, paraffin-embedded tumor sections were immunohistochemically stained for PCNA to estimate the proliferation index (Fig. 7A). YBBEs significantly decreased PCNA expression, the magnitude of change was 59 and 86.3%, respectively, in the 20 and 40 mg/kg YBBEs treated groups (Fig. 7C). On the other hand, the detection of caspase-3 (Fig. 7A and D) and TUNEL (Fig. 7B and E) positive cells for the apoptosis indices indicated more than 3- and 5.5-fold increase of apoptosis by 20 and 40 mg/kg YBBEs treatment. These data therefore support the *in vivo* involvement of

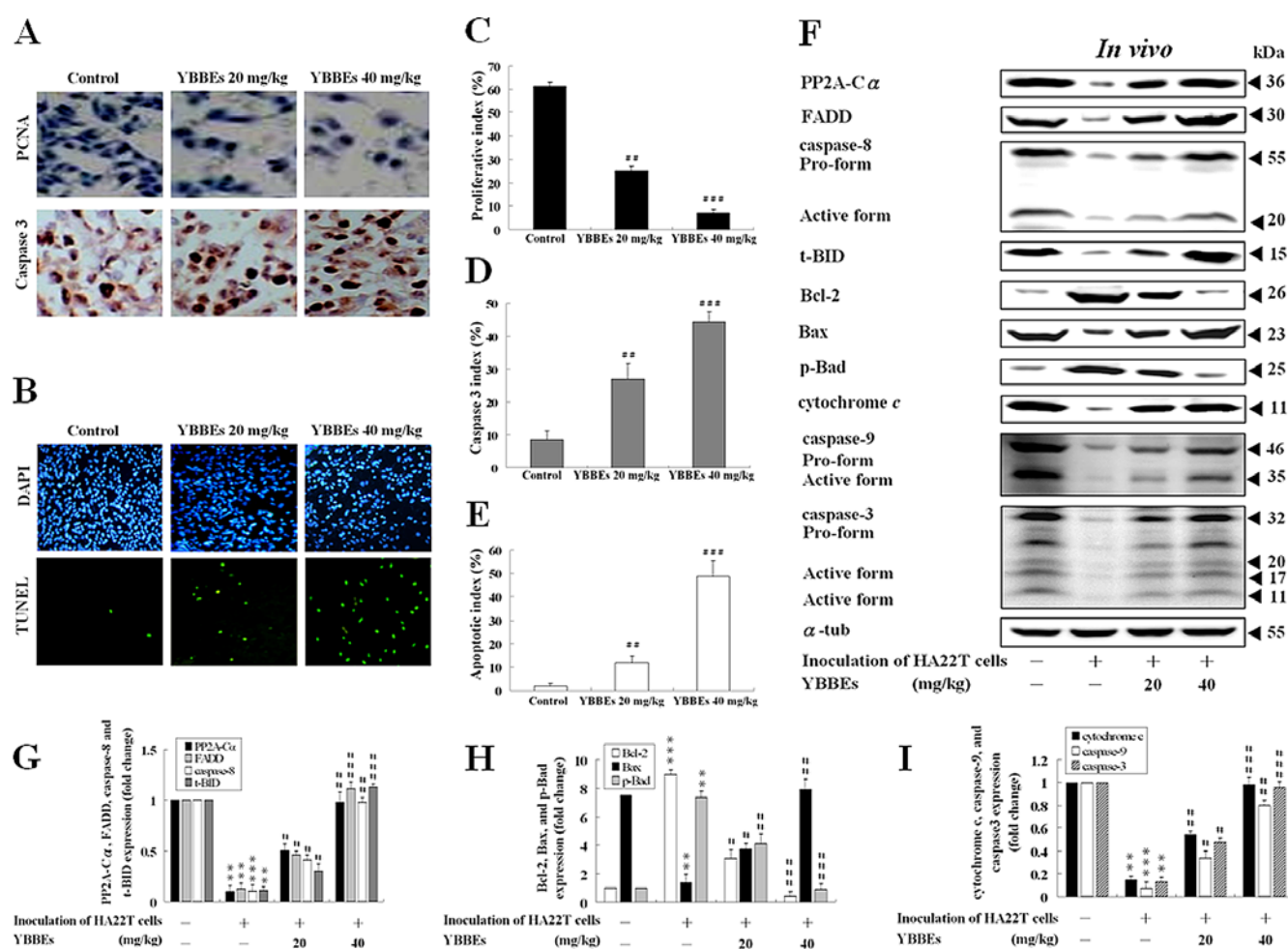


Figure 7. Immunohistochemistry studies and Western blot analysis of tumor tissues treated with different concentrations of YBBEs in HA22T xenograft nude mice model. (A) Representative immunohistochemical stainings for PCNA and caspase-3. (B) Representative immunohistochemical stainings for TUNEL. (C) The proliferative and (D and E) apoptotic indices were calculated by the ratio of positive cells to total number of tumor cells counted. (F) Western blot analysis of the expression levels of different proteins compared to relative values of controls. (G) Bars representing the relative quantification of PP2A-Cα, FADD, caspase-8 and t-BID on the basis of control level. (H) Bars representing the relative quantification of Bcl-2, Bax and p-Bad on the basis of control level. (I) Bars representing the relative quantification of cyt c, caspase-9 and caspase-3 on the basis of control level. Experiments were repeated for five times with similar results. * $p < 0.05$, ** $p < 0.01$ and *** $p < 0.001$ denote significant differences of the groups treated with YBBEs (groups II and III) from the positive control group inoculated with HA22T cells (group I); ** $p < 0.01$ and *** $p < 0.001$ denote significant differences of the positive control group (group I) from the negative control group (mouse without injection of HA22T cells and YBBEs).

caspase-mediated apoptosis as a key contributor of the tumor growth suppression induced by YBBEs. These results are consistent with the *in vitro* results.

Western blot analysis of the expression levels of PP2A-Cα, FADD, caspase-8, t-BID, Bcl-2, Bax, p-Bad, cyt c, caspase-9 and caspase-3 in the tumor cells of the mice treated with different doses of YBBEs is shown in Fig. 7F. In our experiments, the expression levels of PP2A-Cα, FADD, caspase-8, t-BID, Bax, cyt c, caspase-9 and caspase-3 in the tumor cells of mice treated with YBBEs (groups II and III) were higher than those in the tumor cells of the mice of the control group (group I) inoculated with HA22T cells, and the expression levels of PP2A-Cα, FADD, caspase-8, t-BID, Bax, cyt c, caspase-9 and caspase-3 increased when YBBEs concentration increases (Fig. 7F). In addition, the expression levels of Bcl-2 and p-Bad in the tumor cells of the mice of groups II and III were lower than those in the tumor cells of the mice of the control group (group I), and the expression levels of Bcl-2 and p-Bad decreases as YBBEs concentration increases (Fig. 7F). The

in vivo and *in vitro* experimental results are consistent. Thus, YBBEs are able to suppress tumor cell proliferation *in vivo* and to increase tumor cell apoptosis *in vivo*. By virtue of the *in vivo* tests, we preliminarily deduce that YBBEs are effective in liver cancer treatment.

Discussion

Suppression of the apoptotic machinery is a hallmark of cancer development and thus, induction of apoptosis in cancer cells is a useful method for treatment (21). The aim of this study was to evaluate YBBEs, a newly developed herbal medicine as a therapeutic agent for malignant human liver cancer. We found that YBBEs significantly induced apoptosis of HA22T cells both *in vitro* and *in vivo*.

We investigated whether the apoptotic pathway is involved in HA22T cell death caused by YBBEs. Our results confirmed the induction of apoptosis as evident by the presence of membrane blebbing and apoptotic bodies (Figs. 2A and B and 3G).

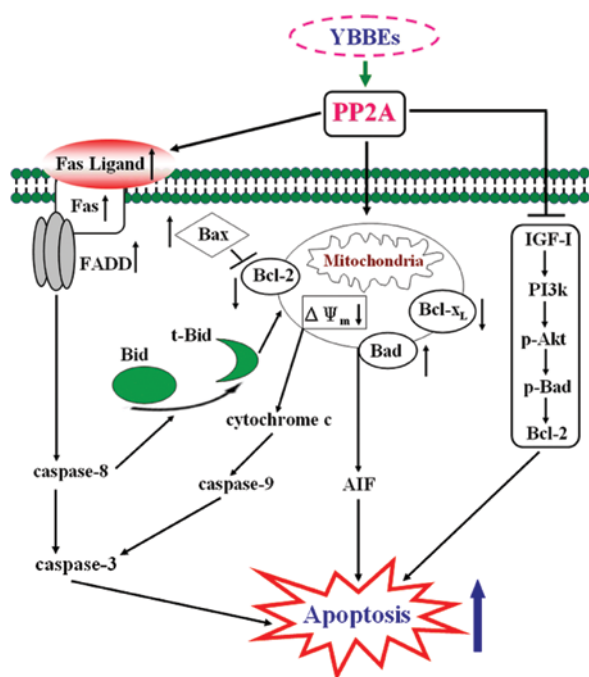


Figure 8. A schematic representation shows the molecular mechanism of YBBEs-induced human HA22T hepatocellular carcinoma cell apoptosis and inhibition of xenografted HA22T tumor growth in nude model. YBBEs induce cell apoptosis in a dose-dependent manner through PP2A, enhance the death receptor and mitochondria-dependent apoptotic pathway, and suppress survival, and expression of the pro-apoptotic Bcl-2 family members.

The apoptotic signaling pathway that leads to caspase activation can be subdivided into two major categories, death receptor-mediated and mitochondria-mediated pathways (22). The death receptors of the tumor necrosis factor (TNF) family such as Fas and TNF-R1 are the best understood death pathways. Recruitment of procaspase-8 through FADD leads to its auto-cleavage and activation, which in turn, activates effector caspases such as caspase-3 (23). YBBEs treatment increased the levels of TNF α , TNF-R1, FAS-L, FAS, FADD, caspase-8, BID and t-BID proteins (Fig. 3A), indicating the involvement of the death-receptor pathway.

Accumulating evidence indicates that the release of cyt c from mitochondria is an important step in apoptosis (24). Alteration in the mitochondrial function in general and induction of the mitochondrial permeability transition in particular plays a key part in apoptosis regulation (25,26). In this study YBBEs disrupted the mitochondrial membrane potential (Fig. 3G), and caused the release of cytochrome c as well as proteolytic activation of caspase-9 and caspase-3 in a dose-dependent manner (Fig. 3E). These results provide evidence that YBBEs caused apoptosis in a human liver cancer cell line through the mitochondria-dependent apoptotic pathway as well.

AIF is a caspase-independent apoptosis effector that can be released from the mitochondria into the cytosol (27-29), and is believed to be involved in caspase-independent cell death (17,18). Correspondingly, our Western blot analysis revealed that treatment of HA22T cells with 0, 50, 100, 150, 200 and 250 μ g/ml YBBEs for 24 h resulted in increased AIF production (Fig. 3E). These findings indicate that the translocation of Bax allows the release of AIF protein from the mitochondria

into the cytosol, which mediates apoptosis through a caspase-independent pathway.

The Bcl-2 family of proteins (pro-apoptotic and anti-apoptotic proteins) and caspases are critical regulators of the apoptotic pathway (30). Reports have demonstrated that translocation of the pro-apoptotic Bax into mitochondria can alter the permeability of cytochrome c, followed by activation of the post-mitochondrial caspase cascade e.g., caspase-9, caspase-8, and caspase-3, leading to apoptotic cell death (31). Consistent with this process, our present study revealed that the treatment of HA22T cells with YBBEs (0, 50, 100, 150, 200 and 250 μ g/ml) for 24 h, markedly decreased the expression of Bcl-2, Bcl-xL and p-Bad proteins, whereas Bax, Bak and Bad protein expression was increased (Fig. 3C). Overexpression of Bax has been reported to accelerate apoptosis, whereas Bcl-2 represses the death function of Bax (32). Thus, increased Bax/Bcl-2 ratio is observed in apoptotic cells (33,34). Our results indicated that YBBEs promoted pro-apoptotic Bax and Bad levels and inhibited the levels of anti-apoptotic Bcl-2 and Bcl-xL; and hence, an increase in the Bax/Bcl-2 ratio occurred (Fig. 3C and D), which may lead to the release of cyt c, procaspase-9 and AIF from the mitochondria to the cytosol, and induce cell apoptosis.

Regulation of cell growth and apoptosis of HCC cells has been shown to be tightly associated with IGF1R signaling (35). It can be speculated that IGF1R inhibition by YBBEs diminishes the mitogenic inputs of the IGF receptor system in HCC cells. Surprisingly, in our experiments, we demonstrated that hepatoma HA22T cells showed high levels of the survival factors IGF-I, p-IGF1R, IGF1R, p-PI3k, PI3k, p-Akt and Akt1. However, following treatment with YBBEs, the expression level of all these proteins was markedly down-regulated (Fig. 4A), which may play a key role in the apoptotic action of YBBEs.

PP2A is a key enzyme in this regulatory network. It is widely distributed throughout the animal and plant kingdoms, and appears to be critical for regulating a number of physiological processes via dephosphorylation of a cohort of specific target proteins (36-38). Inhibition of PP2A by OA results in major cytotoxic effects (39), and the inhibition of PP2A activity at later stages causes mitotic defects (39). Consequently, the specific inhibition of PP2A may promote the cell cycle progression at the start/restriction point (40). Therefore, we further applied the PP2A inhibitor and siRNA assay to examine the role of PP2A involved in YBBEs-induced HA22T cell apoptosis. In the present study, OA totally reversed the YBBEs-mediated up-regulation of FADD, caspase-8, t-BID, Bax, cytochrome c, caspase-9 and caspase-3. In addition, OA reversed the YBBEs mediated down-regulation of Bcl-2 and p-Bad as well (Fig. 5A). These findings suggests that targeting PP2A may be a feasible way to affect the pivotal apoptotic signal pathway. Furthermore, silencing PP2A by RNA-interference blocked the YBBEs-mediated HA22T apoptotic effect, confirming that PP2A is indispensable for mediating the effects of YBBEs (Fig. 5B). Taken together, the *in vitro* findings suggest that YBBEs-induced HA22T apoptosis in a dose-dependent manner mediated through the PP2A. Our current data may provide some significant information for future clinical applications. Moreover, we found that YBBEs dramatically suppressed tumor cell proliferation and induced tumor cell apoptosis in nude mice model (Figs. 6 and 7). The YBBE at a concentration of 40 mg/kg showed a strong effect,

and selectively triggered cancer cell death via inducing the classical apoptotic pathway and suppressing the proliferation of human hepatoma cells *in vivo*. Based on our findings, YBBEs were able to induce human hepatocellular carcinoma HA22T cell apoptosis, which was confirmed using *in vitro* and *in vivo* systems. The possible signaling pathways are shown in Fig. 8.

All our experimental evidence indicates that YBBEs significantly promotes HA22T apoptosis and reduces tumor sizes in xenograft nude mice via PP2A in a dose-dependent manner. In the near future, we would like to further investigate the YBBEs anticancer effect by preclinical studies and clinical trials. Efforts aimed at enhancing YBBEs function and/or activity may provide an alternative therapy for liver cancer.

Acknowledgements

This study was supported by the Taiwan Department of Health Clinical Trial and the Research Center of Excellence (DOH100-TD-B-111-004) and in part by the Taiwan Department of Health Cancer Research Center of Excellence (DOH100-TD-C-111-005).

References

- Okuda K: Hepatocellular carcinoma. *J Hepatol* 32: 225-237, 2000.
- Parkin DM, Bray F, Ferlay J and Pisani P: Estimating the world cancer burden: Globocan 2000. *Int J Cancer* 94: 153-156, 2001.
- Kerr JF, Wyllie AH and Currie AR: Apoptosis: a basic biological phenomenon with wide-ranging implications in tissue kinetics. *Br J Cancer* 26: 239-257, 1972.
- Hill PA, Tumber A and Meikle MC: Multiple extracellular signals promote osteoblast survival and apoptosis. *Endocrinology* 138: 3849-3858, 1997.
- Kawazoe N, Watabe M, Masuda Y, Nakajo S and Nakaya K: Tiam1 is involved in the regulation of bufalin-induced apoptosis in human leukemia cells. *Oncogene* 18: 2413-2421, 1999.
- Mizukami S, Kikuchi K, Higuchi T, Urano Y, Mashima T, Tsuruo T and Nagano T: Imaging of caspase-3 activation in HeLa cells stimulated with etoposide using a novel fluorescent probe. *FEBS Lett* 453: 356-360, 1999.
- Kim SO and Han J: Pan-caspase inhibitor zVAD enhances cell death in RAW246.7 macrophages. *J Endotoxin Res* 7: 292-296, 2001.
- Iizuka N, Miyamoto K, Okita K, Tangoku A, Hayashi H, Yosino S, Abe T, Morioka T, Hazama S and Oka M: Inhibitory effect of Coptidis Rhizoma and berberine on the proliferation of human esophageal cancer cell lines. *Cancer Lett* 148: 19-25, 2000.
- Kao ST, Yeh CC, Hsieh CC, Yang MD, Lee MR, Liu HS and Lin JG: The Chinese medicine Bu-Zhong-Yi-Qi-Tang inhibited proliferation of hepatoma cell lines by inducing apoptosis via G0/G1 arrest. *Life Sci* 69: 1485-1496, 2001.
- Huerta S, Arteaga JR, Irwin RW, Ikezoe T, Heber D and Koefler HP: PC-SPES inhibits colon cancer growth in vitro and in vivo. *Cancer Res* 62: 5204-5209, 2002.
- Zu BX: Whole China herb conglomeration edition. *J People's Public Health* 1: 928-929, 1975.
- Zhang LC: Dictionary of Chinese herbs. *Chao Ren Press* 5: 5513-5514, 1981.
- Hsu H-Y, Chen Y-P, Shen S-J, Hsu C-S, Chen C-C and Chang H-C: *Oriental Materia Medica*. Oriental Healing Arts Institute, Long Beach, CA, pp365-366, 1986.
- Xiang-Ping G-PZ and Shen T: Dictionary of Chinese Herbs. Shanghai Science and Technology Press 2: 3825-3826, 2006.
- Neviani P, Santhanam R, Trotta R, Notari M, Blaser BW, Liu S, Mao H, Chang JS, Galletta A, Uttam A, Roy DC, Valtieri M, Bruner-Klisovic R, Caligiuri MA, Bloomfield CD, Marcucci G and Perrotti D: The tumor suppressor PP2A is functionally inactivated in blast crisis CML through the inhibitory activity of the BCR/ABL-regulated SET protein. *Cancer Cell* 8: 355-368, 2005.
- Alessandri G, Filippeschi S, Sinibaldi P, Mornet F, Passera P, Spreafico F, Cappa PM and Gullino PM: Influence of gangliosides on primary and metastatic neoplastic growth in human and murine cells. *Cancer Res* 47: 4243-4247, 1987.
- Kang YH, Yi MJ, Kim MJ, Park MT, Bae S, Kang CM, Cho CK, Park IC, Park MJ, Rhee CH, Hong SI, Chung HY, Lee YS and Lee SJ: Caspase-independent cell death by arsenic trioxide in human cervical cancer cells: reactive oxygen species-mediated poly(ADP-ribose) polymerase-1 activation signals apoptosis-inducing factor release from mitochondria. *Cancer Res* 64: 8960-8967, 2004.
- Espinosa M, Cantu D, Herrera N, Lopez CM, De la Garza JG, Maldonado V and Melendez-Zajgla J: Inhibitors of apoptosis proteins in human cervical cancer. *BMC Cancer* 6: 45, 2006.
- Hengartner MO: The biochemistry of apoptosis. *Nature* 407: 770-776, 2000.
- Tokunaga E, Oki E, Egashira A, Sadanaga N, Morita M, Kakeji Y and Maehara Y: Deregulation of the Akt pathway in human cancer. *Curr Cancer Drug Targets* 8: 27-36, 2008.
- Kornblau SM: The role of apoptosis in the pathogenesis, prognosis, and therapy of hematologic malignancies. *Leukemia* 12 (Suppl 1): S41-S46, 1998.
- Jin Z and El-Deiry WS: Overview of cell death signaling pathways. *Cancer Biol Ther* 4: 139-163, 2005.
- Thorburn A: Death receptor-induced cell killing. *Cell Signal* 16: 139-144, 2004.
- Reed JC: Cytochrome c: can't live with it - can't live without it. *Cell* 91: 559-562, 1997.
- Green DR and Reed JC: Mitochondria and apoptosis. *Science* 281: 1309-1312, 1998.
- Kroemer G, Dallaporta B and Resche-Rigon M: The mitochondrial death/life regulator in apoptosis and necrosis. *Annu Rev Physiol* 60: 619-642, 1998.
- Chinta SJ, Rane A, Yadava N, Andersen JK, Nicholls DG and Polster BM: Reactive oxygen species regulation by AIF- and complex I-depleted brain mitochondria. *Free Radic Biol Med* 46: 939-947, 2009.
- Hisatomi T, Ishibashi T, Miller JW and Kroemer G: Pharmacological inhibition of mitochondrial membrane permeabilization for neuroprotection. *Exp Neurol* 218: 347-352, 2009.
- Kagan VE, Bayir HA, Belikova NA, Kapralov O, Tyurina YY, Tyurin VA, Jiang J, Stoyanovsky DA, Wipf P, Kochanek PM, Greenberger JS, Pitt B, Shvedova AA and Borisenko G: Cytochrome c/cardioliipin relations in mitochondria: a kiss of death. *Free Radic Biol Med* 46: 1439-1453, 2009.
- Antonsson B and Martinou JC: The Bcl-2 protein family. *Exp Cell Res* 256: 50-57, 2000.
- Kluck RM, Bossy-Wetzel E, Green DR and Newmeyer DD: The release of cytochrome c from mitochondria: a primary site for Bcl-2 regulation of apoptosis. *Science* 275: 1132-1136, 1997.
- Zhao L, Guo QL, You QD, Wu ZQ and Gu HY: Gambogic acid induces apoptosis and regulates expressions of Bax and Bcl-2 protein in human gastric carcinoma MGC-803 cells. *Biol Pharm Bull* 27: 998-1003, 2004.
- Fan J, Li R, Zhang R, Liu HL, Zhang N, Zhang FQ and Dou KF: Effect of Bcl-2 and Bax on survival of side population cells from hepatocellular carcinoma cells. *World J Gastroenterol* 13: 6053-6059, 2007.
- Salakou S, Kardamakis D, Tsamandas AC, Zolota V, Apostolakis E, Tzelepi V, Papathanasopoulos P, Bonikos DS, Papapetropoulos T, Petsas T and Dougenis D: Increased Bax/Bcl-2 ratio up-regulates caspase-3 and increases apoptosis in the thymus of patients with myasthenia gravis. *In Vivo* 21: 123-132, 2007.
- Ellouk-Achard S, Djenabi S, De Oliveira GA, Desauty G, Duc HT, Zohair M, Trojan J, Claude JR, Sarasin A and Lafarge-Frayssinet C: Induction of apoptosis in rat hepatocarcinoma cells by expression of IGF-I antisense c-DNA. *J Hepatol* 29: 807-818, 1998.
- Vintermyr OK, Mellgren G, Boe R and Doskeland SO: Cyclic adenosine monophosphate acts synergistically with dexamethasone to inhibit the entrance of cultured adult rat hepatocytes into S-phase: with a note on the use of nucleolar and extranucleolar [³H]-thymidine labelling patterns to determine rapid changes in the rate of onset of DNA replication. *J Cell Physiol* 141: 371-382, 1989.
- Kinoshita N, Ohkura H and Yanagida M: Distinct, essential roles of type 1 and 2A protein phosphatases in the control of the fission yeast cell division cycle. *Cell* 63: 405-415, 1990.
- Lewin B: Driving the cell cycle: M phase kinase, its partners, and substrates. *Cell* 61: 743-752, 1990.
- Cohen P, Holmes CF and Tsukitani Y: Okadaic acid: a new probe for the study of cellular regulation. *Trends Biochem Sci* 15: 98-102, 1990.
- Cohen P: Classification of protein-serine/threonine phosphatases: identification and quantitation in cell extracts. *Methods Enzymol* 201: 389-398, 1991.